

Geometrical properties of rock joints and their effects on rock mechanical behaviour

Authors: Dr. Wasantha Pallewela Liyanaga Piyal, Prof. Dr. habil. Heinz Konietzky
(TU Bergakademie Freiberg, Geotechnical Institute)

1	Introduction.....	2
2	Major joint geometrical properties.....	2
2.1	Joint orientation	2
2.2	Joint persistence	7
2.3	Joint degree of interconnectivity	9
2.4	Surface roughness	12
3	Conclusions and recommendations.....	16
4	References	16

1 Introduction

The strength of the rock mass is the single most important parameter for the design of structures in or on rock masses. Therefore, accurate determination of rock mass strength is the cornerstone for the safe and economical implementation of rock mechanics and rock engineering projects such as open-pit mines, tunnels, drifts and rock caverns. Rock is inherently heterogeneous, owing to the presence of discontinuities. Discontinuities can occur in the form of joints, faults, fissures, bedding, etc. Nevertheless, the term 'joint' is generally used in rock mechanics to represent all types of discontinuities. Joints are the planes of weakness in rock masses and can be found in various geometrical shapes, depending on past geological processes. These joint geometrical properties (such as persistence, orientation, degree of interconnectivity, surface roughness) can have a marked influence on the strength and other mechanical properties of rock masses. This chapter briefly discusses the existing knowledge related to the influence of some major joint geometrical properties on rock mechanical behavior and highlights some recommendations for future research studies in order to better understand the mechanical behaviour of rock masses.

2 Major joint geometrical properties

Geometrical properties refer to the different characteristics of the spatial arrangement of joint/joints within a rock mass. When considering unfilled matched joints, there are four geometrical properties of interest, which are known to have a significant influence on rock mechanical behavior: joint orientation, persistence (length), degree of interconnectivity and surface roughness (see Fig. 1). The following sub-sections discuss in detail the influences of these four different joint geometrical properties on rock mechanical behavior.

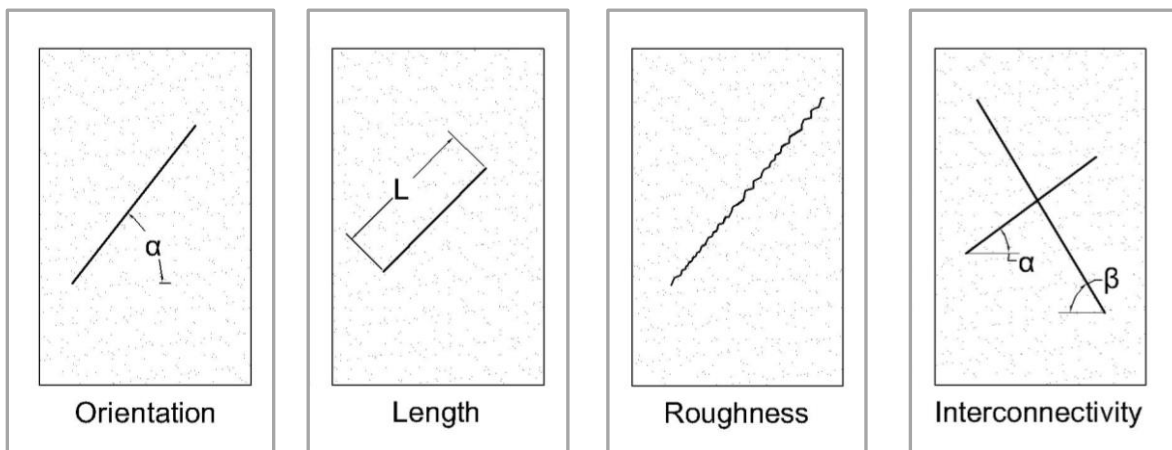


Fig. 1: Some of the major joint geometrical properties

2.1 Joint orientation

The orientation, sometimes known as the angle, of a joint can be measured with respect to the major or minor principal stress direction. Jaeger (1959) provided theoretical descriptions for the influence of joint orientation on the strength of a rock mass. His theoretical model considers a jointed rock comprising intact rock material and a single, fully-persistent joint subjected to major and minor principal stresses. Two separate equations, one to characterize the conditions of failure where failure proceeds by sliding along the pre-existing joint (slippage) (Eq. 1) and another to characterize failure through

the intact material (Eq. 2), were derived in Jaeger et al. (2007). Equation 1 defines ‘sliding plane of weakness’ theory.

$$\sigma_1 = \sigma_3 + \frac{2(S_w + \mu_w \sigma_3)}{(1 - \mu_w \cot \beta) \sin(2\beta)} \quad (1)$$

$$\sigma_1 = 2S_0 \tan \beta + \sigma_3 \tan^2 \beta \quad (2)$$

where σ_1 is the major principal stress, σ_3 is the minor principal stress, S_w is the joint cohesion, μ_w is the joint friction coefficient ($\mu_w = \tan \phi_w$ where ϕ_w is the joint friction angle), S_0 is the cohesion of the intact material and β is the joint orientation measured from the minor principal stress direction. Jaeger et al. (2007) gave the condition for slippage on the considered plane of weakness as:

$$|\tau| = S_0 + \mu \sigma \quad (3)$$

Where $|\tau|$ is the shear strength of the joint and σ is the normal stress. The stress state representation on a Mohr-Coulomb diagram (based on the Mohr-Coulomb theory, Coulomb (1776) and Mohr (1900)), relevant to Eq. 1, was also presented in Jaeger et al. (2007) (Figure 2), with the condition related to Equation 3 represented by a straight line oriented at angle β to the σ axis (refer to the PQR line in Fig. 2).

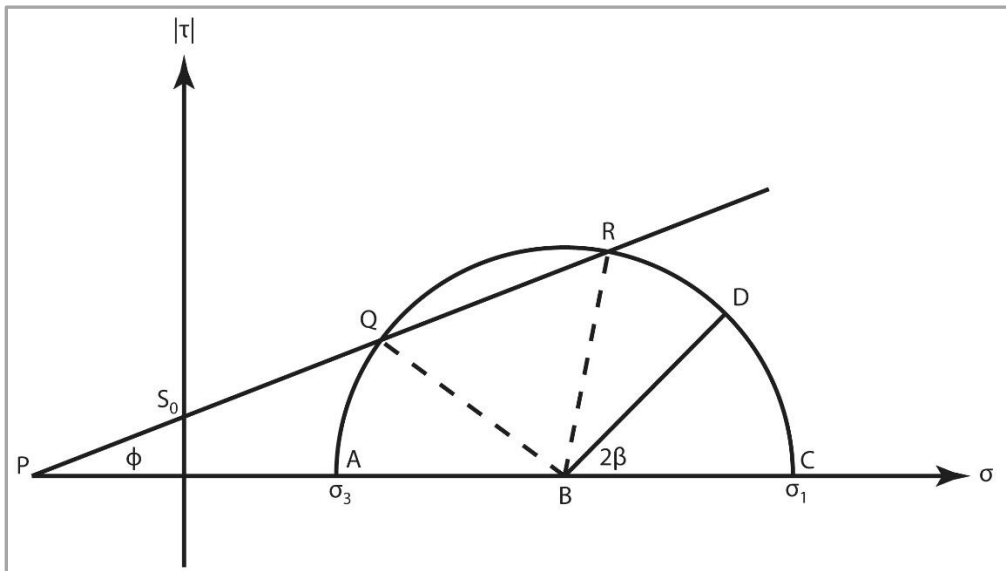


Fig. 2: Mohr-Coulomb diagram representation for the stress state defined in Equation 1 (after Jaeger et al. 2007).

Jaeger et al. (2007) stated that slippage on a joint can only occur for values of β which place the point D of Fig. 2 within the arc defined by the intersects between the Mohr's circle and points Q and R. Thus, for increasing β , slippage will first be initiated when point D coincides with point R (when $\beta = \phi_w$) and will cease when point D coincides with point Q.

For the scenario depicted by Eq. 1, the minimum strength of the jointed rock σ_1^{\min} , can be calculated from Eq. 4, and occurs for a critical joint orientation, β_w given by Eq. 5 (Jaeger et al. 2007):

$$\sigma_1^{\min} = \sigma_3 + 2(S_w + \mu_w \sigma_3) \left[(1 + \mu_w^2)^{1/2} + \mu_w \right] \quad (4)$$

$$\tan 2\beta_w = -1/\mu_w \quad (5)$$

For the situation encountered in UCS testing, σ_3 can be considered negligible, resulting in the description given by Eq. 6 for the minimum strength of jointed rock:

$$\sigma_1^{\min} = 2S_w \left[(1 + \mu_w^2)^{1/2} + \mu_w \right] \quad (6)$$

From Eq. 5, it can be seen that the critical joint orientation in sliding plane of weakness theory is dependent on the friction angle of the joint, and equal to $(45 + \frac{\phi_w}{2})$. Eq. 1 shows that rock strength will increase with decreasing joint angle (β) for joint angles less than $(45 + \phi_w/2)$ and increasing joint angle β for joint angles greater than $(45 + \phi_w/2)$. Eq. 1 also demonstrates that the nature of rock strength variation with joint angle is dependent on both joint friction angle and cohesion. Fig. 3 depicts a family of curves representing joints with different friction angles in the UCS/joint cohesion vs. joint angle space. Two plots showing the same curves are provided in Fig. 3, to demonstrate how the theoretical curves appear with differing magnification of the vertical axis. Variation in joint cohesion will influence the scale of the vertical axis in Fig. 3, but not the fundamental shape of the curves.

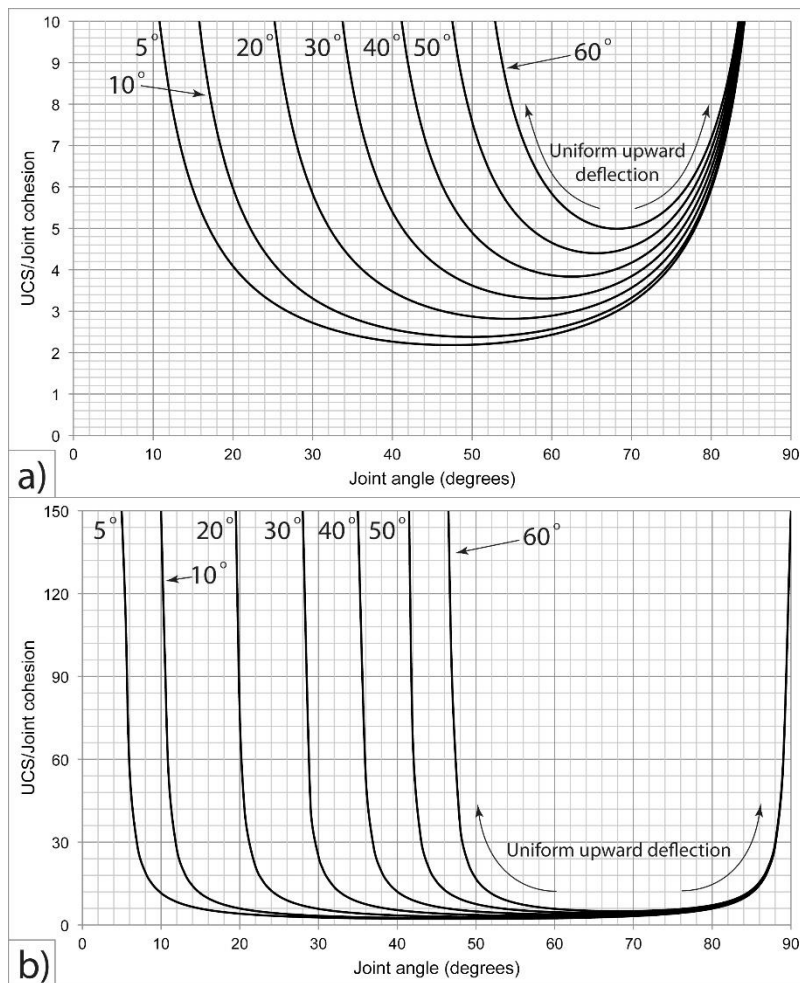


Fig. 3: Theoretical curves for joints with various values of friction angle ϕ_w in UCS/joint cohesion vs. joint angle space.

The curves of Fig. 3 display a form defined by a progressive increase in the rate of UCS increase with increasing joint orientation, for joint orientations greater than the critical value (see arrows on Fig. 3). Exactly the same progressively increasing rate of UCS increase can also be observed with decreasing joint orientation, for joint orientations less than the critical value (see arrows on Fig. 3). These features can be described as ‘uniform upward deflection’ features that occur with distance from the position of the critical joint angle on the horizontal axis. The theoretical curves are perfectly symmetrical about a vertical line through the critical joint orientation. For all cases, the theoretical curve becomes infinitely steep as it approaches joint orientations of ϕ_w and 90° (i.e. a vertical joint). The joint friction angle influences the width of the horizontal axis that the curve occupies, in addition to the location of the critical point on both the horizontal and vertical axes (Fig. 3). The joint cohesion influences the position and form of the curves relative only to the vertical axis. A typical variation of strength against joint orientation, according to Eq. 1, is shown in Fig. 4.

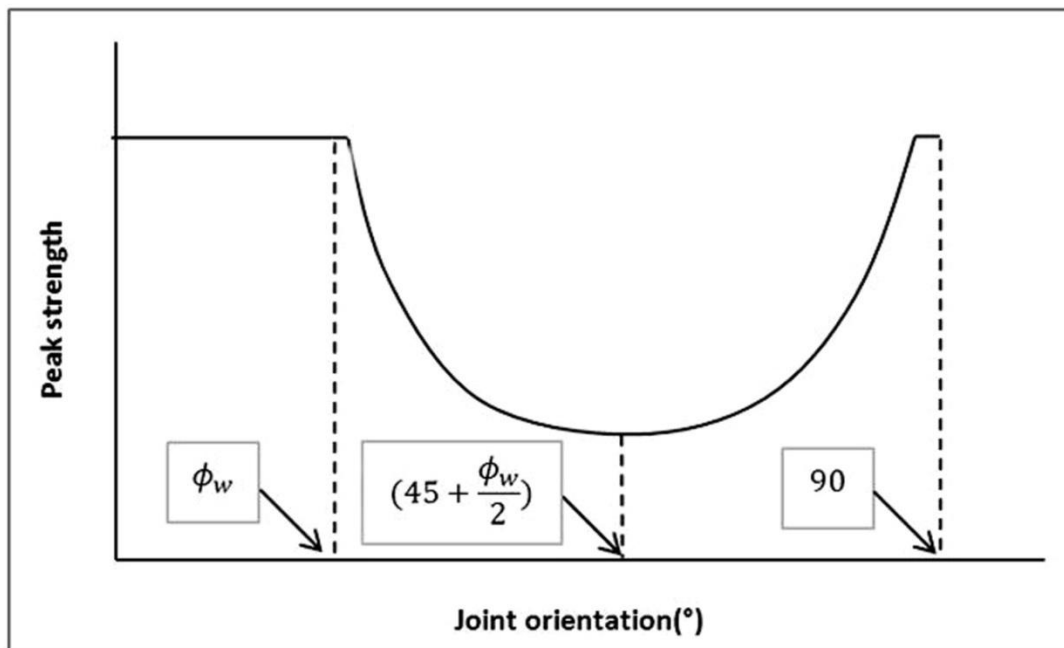


Fig. 4: Peak strength vs. joint orientation according to the sliding plane of weakness model

There are three important observations that can be made from Eq. 1 and Fig. 4.

1. There is no influence from the joint on strength for joint orientations between 0 and ϕ_w .
2. The minimum strength (the maximum influence from the joint) occurs for a joint orientation of $(45 + \phi_w/2)$
3. When the joint is oriented at an angle of 90°, strength is not influenced by the joint

A number of previous research studies have shown that the variation of strength against joint orientation is consistent with the sliding plane of weakness model of Jaeger et al. (2007) (c.f. Yang et al., 1998; Kulatilake et al., 2001; Singh et al., 2002; Ranjith et al., 2004; Kumar and Das, 2005; Tiwari and Rao 2004; Ramamurthy and Arora 1994; Wasantha et al. 2011; Wasantha et al. 2014). Triaxial experiments by Ramamurthy and Arora (1994) showed that increasing confining pressure decreases the influence of joint orientation on strength of rock, as the higher normal stress acting on the joint at higher confining pressures imposes a greater resistance to joint sliding (Fig. 5a). Wasantha et al. (2014) conducted triaxial experiments under undrained triaxial stress conditions and also found a variation of strength against joint orientation that is supportive of the sliding plane of weakness model of Jaeger et al. (2007) (Figure 5b).

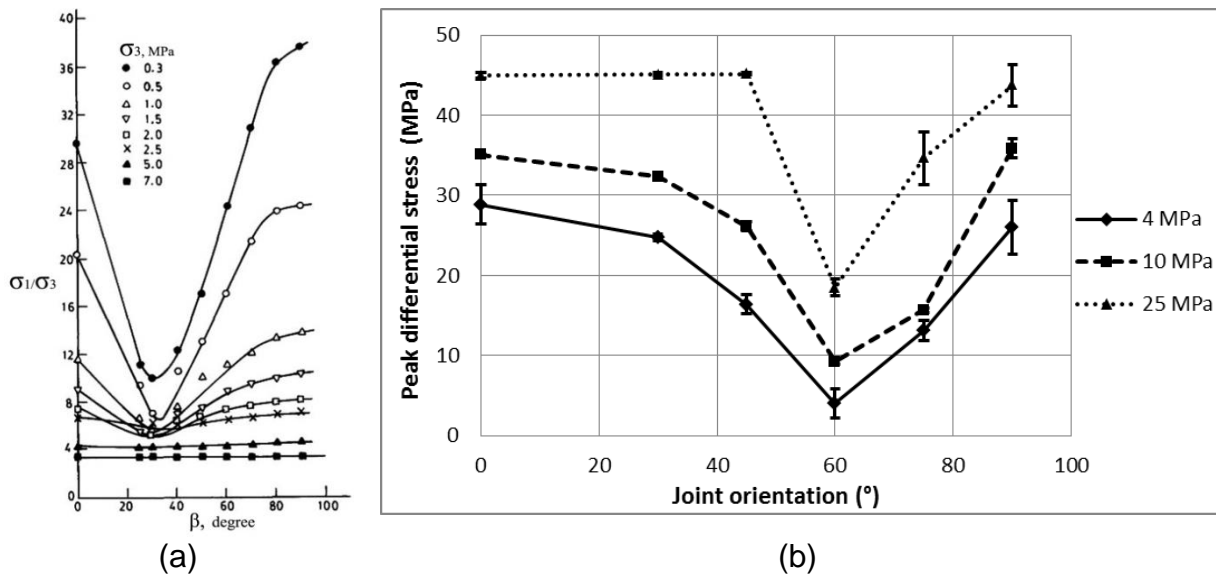


Fig. 5: Strength vs. joint orientation under different confining pressures after (a) Ramamurthy and Arora (1994) and (2) Wasantha et al. (2014)

While the results of many previous studies are consistent with the sliding plane of weakness model of Jaeger et al. (2007), results of some other studies do not completely agree with it. For example, the experiments of Dunn et al. (1973) on four different types of bedded sandstones (Navajo, Catawba Quartzite, Kayenta and Cutler sandstone) revealed that only Navajo and Catawba Quartzite sandstone show minimum fracture strength at 30° orientation (measured from the compression direction) and there is no systematic variation of fracture strength against bedding orientation for other types of sandstones. Furthermore, Baud et al. (2005) observed that the peak strength does not dip to a minimum at intermediate bedding angles for porous sandstones as it does for foliated rocks or shale.

2.2 Joint persistence

The persistence of joints is usually estimated based on the trace length of the joint. A typical schematic demonstration of persistent and non-persistent joints is shown in Fig. 6, as described in Kim et al. (2007a).

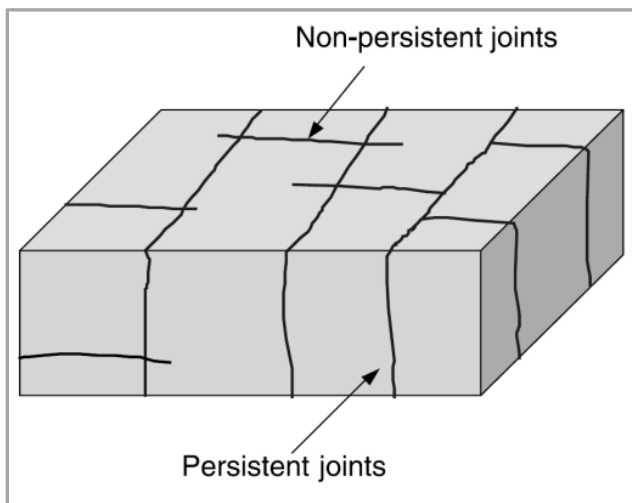


Fig. 6: Persistent joints versus non-persistent joints (after Kim et al. 2007a)

In the opinion of Kim et al. (2007a), joint persistence, or the relative size of the joint, is of equal importance to other joint geometrical properties (such as orientation and degree of interconnectivity) for the mechanical behaviour of jointed rock masses. Relative to intact rock, joints form the weaker component of jointed rock masses. A decrease in joint persistence will increase the proportion of rock mass dominated by intact rock (relative to joints) and thus should strengthen the jointed rock mass and enhance its stability. Einstein et al. (1983) carried out a study on the influence of the persistence of discontinuities on slope stability, providing a set of empirical recommendations for the treatment of joint persistence in rock slope design. Kim et al. (2007a) further emphasized that the presence of non-persistent joints has a significant effect on the properties and behavior of rock masses, and therefore stated that the persistence of rock joints should be considered in engineering characterization of rock masses.

Halakatevakis and Sofianos (2010) presented a model to determine the shear strength of a non-persistent joint in terms of that of an equivalent fully-persistent joint (Eq. 7):

$$\tau = C_t + \sigma_n \tan \varphi_t = [X \cdot C_w + (1 - X)C_i] + \sigma_n \cdot [X \cdot \tan \varphi_w + (1 - X)\tan \varphi_i] \quad (7)$$

Where, C_t and φ_t are the cohesion and angle of internal friction of the equivalent fully-persistent discontinuity, respectively, C_w, φ_w are the cohesion and angle of internal friction of the original non-persistent discontinuity, respectively, C_i, φ_i are the cohesion and angle of internal friction of the intact rock and X is the persistence of the discontinuity. The model of Halakatevakis and Sofianos (2010) has also been validated by them using numerical experiments.

The Geological Strength Index (GSI), a measure commonly used to describe the influence of joints on rock strength in engineering, does not directly account for joint persistence. Cai et al. (2007) presented a model, as shown in Eq. 8, to determine the GSI to be used with the Hoek-Brown failure criterion (Hoek et al. 1995; Hoek et al. 2002). Their model uses block volume V_b and a joint surface condition factor J_c to determine the GSI.

$$GSI(V_b, J_c) = \frac{26.5 + 8.79 \cdot \ln J_c + 0.9 \cdot \ln V_b}{1 + 0.0151 \cdot \ln J_c - 0.0253 \cdot \ln V_b} \quad (8)$$

Where, V_b and J_c should be determined using following two equations, respectively:

$$V_b = \frac{S_1 S_2 S_3}{\sin \gamma_1 \sin \gamma_2 \sin \gamma_3 \sqrt[3]{P_1 P_2 P_3}} \quad (9)$$

$$J_c = \frac{J_w J_s}{J_A} \quad (10)$$

Where S_j , γ_j , P_j are the joint spacing, the orientation between joint sets and the joint persistent factor, respectively, and J_W , J_S , J_A are the joint large-scale waviness factor, small-scale smoothness factor and alteration factor, respectively.

Kim et al. (2007b) demonstrated variation in the ratio of GSI calculated considering joint persistence to GSI calculated neglecting joint persistence and the ratio of rock mass strength calculated considering persistence to rock mass strength calculated without considering the persistence against joint persistence, using statistical simulations (Fig. 7a and b). Their results showed that for jointed rock masses where joint persistence is low, consideration of the persistence of rock joints significantly influences calculated rock mass properties obtained, but for jointed rock masses where joint persistence is high, consideration of the persistence of rock joints is less important.

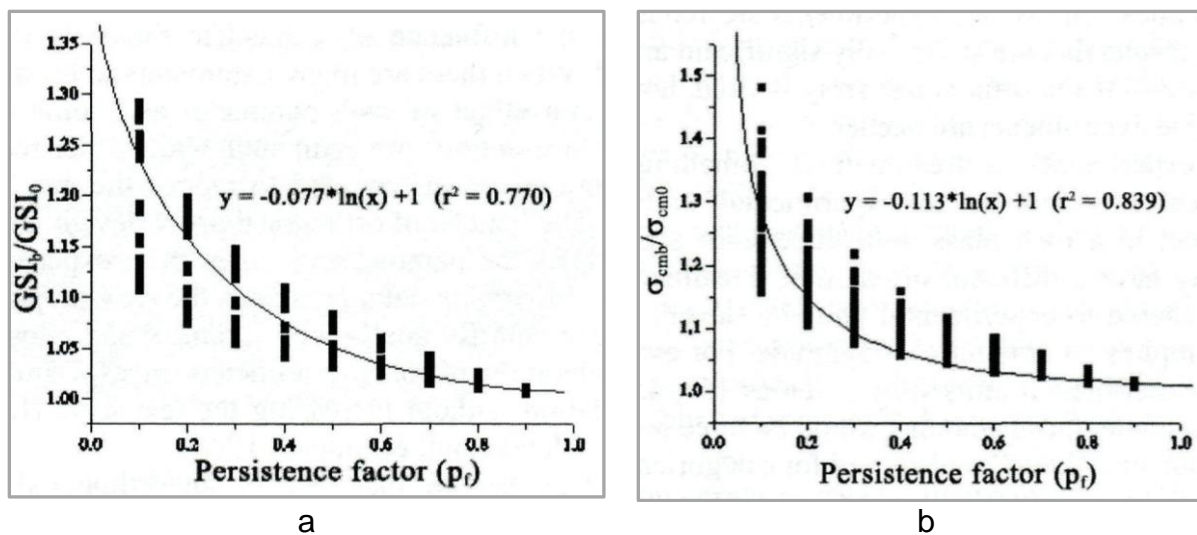


Fig. 7: (a) Ratio of GSI vs. Persistence factor, (b) Ratio of rock mass strength vs. Persistence factor (Kim et al. 2007b)

2.3 Joint degree of interconnectivity

Joints in heavily jointed rock masses often intersect. Intersecting joints/joint sets can take one of two broad patterns, with each defined by the relative orientation of the two intersecting joints/joint sets when viewed in 2D. When the orientations of the joints/joint sets are such that both have the same dip (from the horizontal), but different dip directions, the interconnectivity is termed symmetric (Fig. 8). When the intersecting joints/joint sets have different dips, the interconnectivity is termed skew-symmetric (Fig. 8). Two intersecting, fully-persistent joints will delineate four discrete blocks. One edge of each of these blocks will meet at the 'joint junction point'. This edge is denoted here as the 'tip' of the block.

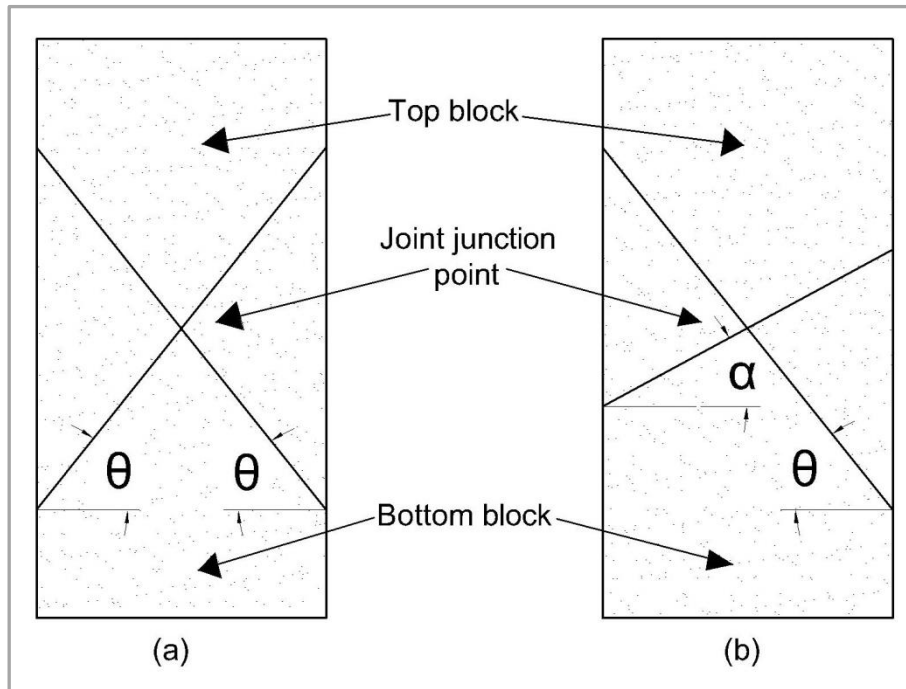


Fig. 8: Joint configurations for a doubly-jointed sample with (a) symmetric interconnectivity, and (b) skew-symmetric interconnectivity

A thorough understanding of the expected mechanical response of rock to loading under intact, singly- and multiply-jointed rock scenarios (including the two scenarios depicted in Fig. 8) is extremely important for the design of rock structures.

Rouleau and Gale (1985) proposed an empirical index value to evaluate the degree of interconnectivity between two joint sets (Eq. 11).

$$I_{ij} = \frac{l_i}{S_j} \sin \gamma_{ij} \quad (i \neq j) \quad (11)$$

where, I_{ij} is the interconnectivity index, l_i is the mean trace length for set i , S_j is the mean spacing for set j and γ_{ij} is the average angle between joint sets i and j .

It should be noted that Eq. 11 was not derived on the basis of any theoretical considerations (i.e. it is entirely empirical), and was suggested simply as a mean of incorporating joint orientation, trace length and spacing data in a method for the characterization of the interconnectivity of a joint network.

Although many experimental studies have been carried out on rock with a single joint or joint set, few experimental studies have considered rock masses with multiple, interconnected joints/joint sets (Yang et al. 1998; Kulatilake et al. 2001; Chong et al. 2013). Yang et al. (1998) tested rectangular prismatic samples made of a plaster-sand mixture that contained rough joint sets in systematically varying orientations across the sample set. Their samples were $125 \times 100 \times 300$ mm in size and samples with two and three joint sets were considered (Fig. 9). Their testing considered only uniaxial compression. Eight different combinations of interconnected joint set orienta-

tions were used, of which five considered symmetric interconnectivity (i.e. $0^\circ/90^\circ$, $15^\circ/-15^\circ$, $30^\circ/-30^\circ$, $40^\circ/-40^\circ$, $45^\circ/-45^\circ$, $60^\circ/-60^\circ$, $15^\circ/-30^\circ$, $15^\circ/-45^\circ$).

Kulatilake et al. (2001) conducted a series of UCS tests on jointed samples also made of a plaster-sand mixture. Their samples were 300 x 125 x 86 mm in size and contained two interconnected joint sets, with different combinations of joint orientations ranging from 0° to 40° (creating both symmetric and skew-symmetric interconnectivities).

Chong et al. (2013) provided numerical modeling results that contrast with the experimental results of Yang et al. (1998) and Kulatilake et al. (2001). Their study used the three-dimensional Distinct Element Code (3DEC) to perform numerical simulation of triaxial loading of specimens with a single joint with various orientations, and two interconnected joints with various orientations (but only symmetric interconnectivity, for which dip directions for the joint pair were toward one another) (Fig. 10).

Wasantha et al. (2014) further discusses effect of joint interconnectivity on rock mechanical behaviour with their experimental findings.

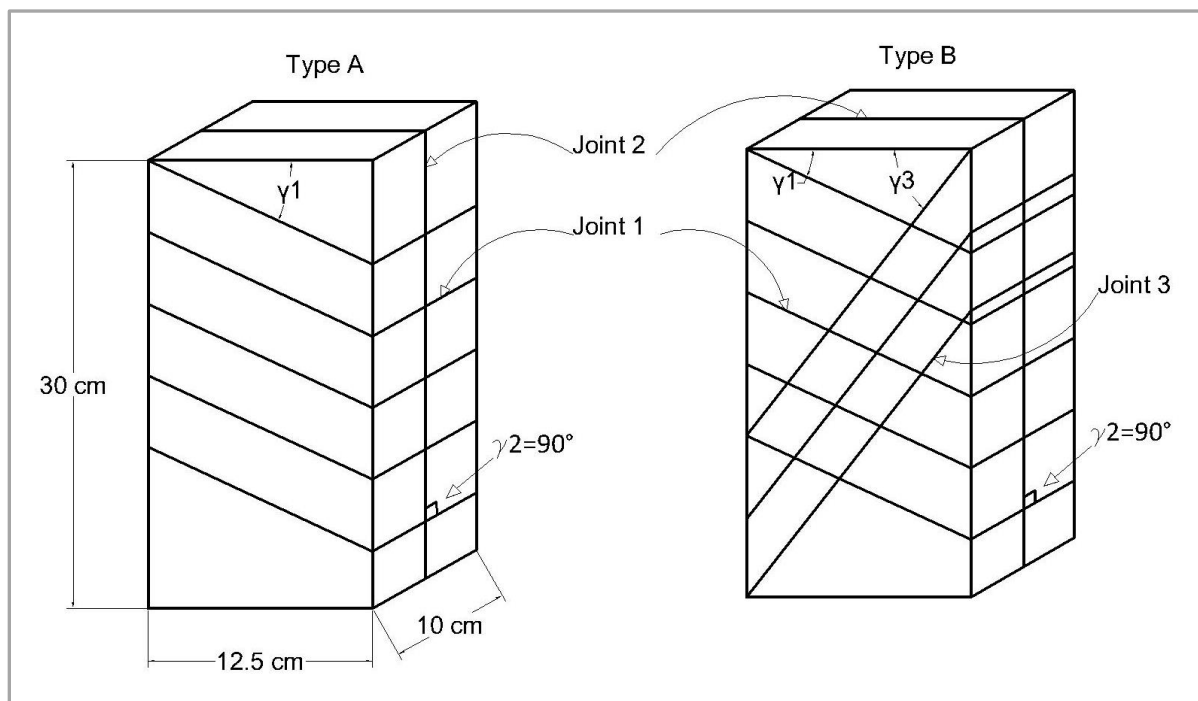


Fig. 9: Rock mass models produced for testing with two joint sets (Type A) and three joint sets (Type B) (after Yang et al. 1998)



Fig. 10: Images of failed specimens for the (a) single-joint model, and (b) double-joint model of Chong et al. (2013) (the non-blue colour areas denote shear/tensile failure within intact material)

2.4 Surface roughness

The surface roughness of joints directly influences their shear strength. The shear strength of joints is usually considerably lower than the shear strength of intact rock and their tensile strength is negligible. Several shear strength models can be found in the research literature to determine the shear strength of joints. However, most of the studies in the literature have considered idealized rock joints (i.e. either planar or regular saw-toothed rock joints).

The Mohr-Coulomb failure criterion can also be applied to joints to calculate their shear strength, and the relevant equation is shown below (Eq. 12).

$$\tau = c_j + \sigma_n \tan \phi_j \quad (12)$$

where, τ is the shear stress along the contact surface at failure, c_j is the joint cohesion, σ_n is the normal stress and ϕ_j is the joint friction angle.

The Mohr-Coulomb model assumes that the joint surface is plain and smooth, which is however not the case in joints found in the field. Natural joints often contain asperities and these asperities can be of two orders: (1) first-order asperities that account for the waviness of the joint profile and (2) second-order asperities that account for the unevenness of the joint profile. Therefore, the shear strength-normal stress relationship is non-linear for such natural joints. By taking the asperity inclination angle into consideration, Patton (1966) presents a bilinear shear strength model (Eq. 13).

$$\tau = \sigma_n \tan(\phi_b + i) \quad (13)$$

Where, ϕ_b is the basic friction angle, and i is the asperity inclination angle. At higher normal stresses, the peak shear strength criterion in Eq. 13 changes to Eq. 14.

$$\tau = c + \sigma_n \tan \phi_r \quad (14)$$

Where ϕ_r is the residual friction angle. Eq. 13 and 14 of Patton's (1966) model represent two straight lines with different gradients on the space of shear strength versus normal stress (Fig. 11). To provide a smooth transition between these two linear variations, Jaeger (1971) proposed a new shear strength model (Eq. 15):

$$\tau = c_a (1 - e^{-d\sigma_n}) + \sigma_n \tan \phi_r, \quad (15)$$

where d is an experimentally determined empirical parameter. Typical curves for the shear strength models represented by Eq. 13, 14 and 15 are shown in Fig. 11. More studies of the shear strength of joints with saw-toothed surfaces have been carried out by many researchers including Saeb (1990), Homand et al. (1999), Haque and Kodikara (2012), Xia et al. (2013), Kulatilake et al. (1995), and Haberfield and Johnston (1994).

Since natural rock joints are often neither planar nor saw-toothed, none of the above models truly integrates the characteristics of natural joint profiles for estimating shear strength. Barton and his co-workers (Barton 1976; Barton and Choubey 1977; Barton and Bandis 1990) addressed this issue by proposing a new shear strength model with the facility to incorporate the roughness of irregular joint surfaces through a roughness coefficient called the Joint Roughness Coefficient (JRC). With their shear strength model, they provided ten different standard joint profiles with different JRC values ranging from 0 to 20, to compare and estimate the JRC values of real joints. Eq. 16 shows this shear strength criterion and Fig. 12 displays the ten different standard joint profiles with their appointed JRC values.

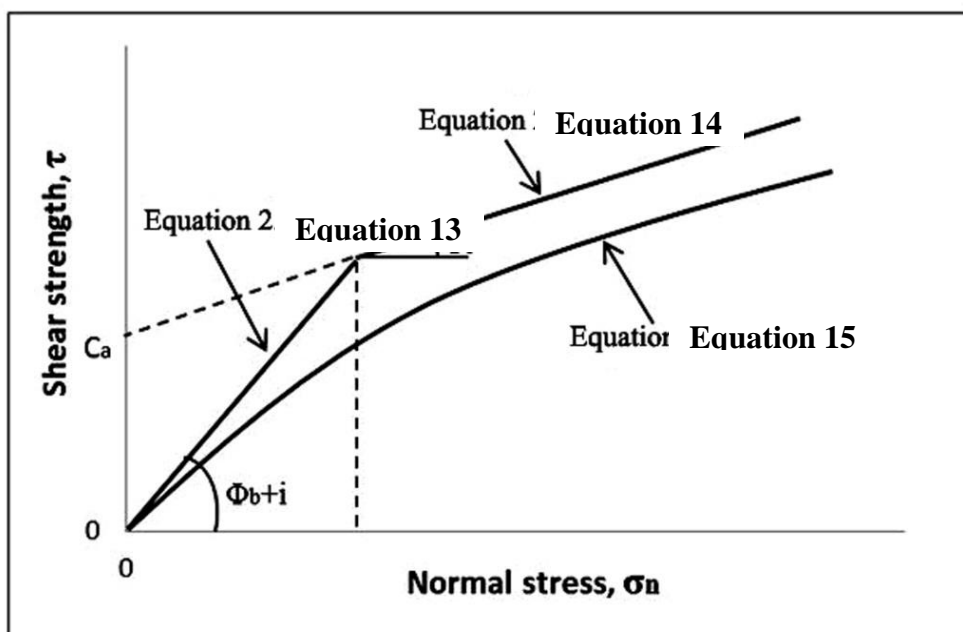


Fig. 11: Shear strength versus normal stress curves for different shear strength models

$$\tau = \sigma_n \tan \left(JRC \cdot \log \left(\frac{JCS}{\sigma_n} \right) + \phi_r \right) \quad (16)$$

As Eq. 16 suggests, three factors control the shear strength of joints: (1) residual friction angle ϕ_r (2) geometry of surface profile, JRC and (3) asperity failure component JCS/σ_n . Of these three factors, JRC and JCS are scale-dependent. Therefore, Barton and Bandis (1982) proposed scale corrections for these two factors, after extensive experimentation and review of the literature on rock joints, as shown in Eq. 17 and 18.

Profile	JRC
	0-2
	2-4
	4-6
	6-8
	8-10
	10-12
	12-14
	14-16
	16-18
	18-20

Fig. 12: Different joint surface profiles with their appointed JRC values (after Barton and Choubey 1977)

$$JRC_n = JRC_0 \left[\frac{L_n}{L_0} \right]^{-0.02 JRC_0} \quad (17)$$

$$JCS_n = JCS_0 \left[\frac{L_n}{L_0} \right]^{-0.03 JCS_0} \quad (18)$$

Where, JRC_n is the joint roughness coefficient relevant to in-situ block, JCS_n is the joint wall compressive strength relevant to in-situ block, JRC_0 is the joint roughness coefficient relevant to laboratory-scale specimen, JCS_0 is the joint wall compressive strength relevant to laboratory-scale specimen, L_n is the length of a joint in an in-situ block and L_0 is the length of a joint in a laboratory-scale specimen.

Barton (1976) cautioned that for effective normal stresses greater than the UCS of the rock material, shear strength predictions using Eq. 16 may be appreciably smaller than the actual shear strengths. Moreover, the subjective nature of this criterion (i.e. assigning JRC values for real rock joints depends on the experience of the user) is another concern among practitioners.

Lee et al. (2006) proposed a new peak shear strength criterion, as shown in Eq. 19, that replaces the JRC of the Barton's model (Eq. 16) with surface roughness parameter R_s :

$$\tau = \sigma_n \tan \left((169.2 \cdot \ln R_s + 9.1) \log \left(\frac{JCS}{\sigma_n} \right) + \phi_b \right) \quad (19)$$

Grasselli and Egger (2003) suggested a new constitutive law for the shear strength of rock joints based on three-dimensional surface parameters and Eq. 20 depicts this model.

$$\tau = \sigma_n \tan \left(\phi_b + \left(\frac{\theta_{\max}^*}{C} \right)^{1.18 \cos \alpha} \right) \left(1 + e^{-\left(\frac{\theta_{\max}^*}{9A_0 C} \right) \left(\frac{\sigma_n}{\sigma_t} \right)} \right) \quad (20)$$

Where θ_{\max}^* is the maximum apparent dip angle in the shear direction, C is a 'roughness' parameter, A_0 is the maximum possible contact area in the shear direction and σ_t is the tensile strength.

There have been several other peak shear strength models developed in the literature considering various types of rock joints, however most of them are with significant limitations.

3 Conclusions and recommendations

The geometrical properties of joints significantly influence the mechanical behaviour of rock masses and numerous theoretical, experimental and numerical studies have consistently shown this. This chapter discusses the effect of four major joint geometrical properties – orientation, persistence, degree of interconnectivity and surface roughness – on rock mechanical behaviour. Joint orientation is a crucial parameter in deciding the failure mechanisms of rock masses; i.e. failure along the joint vs. failure through the intact rock matrix. The persistence effect of joints is straightforward, and a long weaker joint plane decreases the rock mass strength to a relatively greater extent than a relatively shorter joint plane. Nevertheless, to date the non-persistent nature of joints has not been sufficiently integrated into stability assessments of rock masses. In heavily jointed rock masses, joints often intersect with each other. The degree of interconnectivity of these joints can cause complex mechanical responses of rock masses. Even though the influence of the degree of joint interconnectivity on rock mass behavior is known to be critical, disappointingly few studies have been reported on this topic in the literature. Shear behaviour of rough rock joints has been studied by numerous researchers and some models have been derived to describe it. However, the nature of pore-water pressure fluctuation along the joints during shearing and its secondary influences on shear behaviour have not been thoroughly studied to date.

Various rock mass strength models are generally used to estimate the strength of rock. Of these, the Hoek-Brown failure criterion is amongst the most popular. However, the vast majority of these models do not effectively take the effect of the geometrical properties of joints on rock mass strength into account. Therefore, a better approach that satisfactorily accounts for the joint geometrical properties is a priority research need in order to more faithfully estimate the strength of rock masses.

4 References

- Barton N (1976). The shear strength of rock and rock joints. *Int. J. Rock Mech. Min. Sci. Geomech. Abstr.*, 13: 255 - 279.
- Barton NR, Bandis SC (1982). Effects of block size on the shear behavior of jointed rock. 23rd U.S. Symp. on Rock Mech., Berkeley, 739 - 760.
- Barton N, Bandis SC (1990). Review of predictive capabilities of JRC-JCS model in engineering practice. *Proc. of the Int. Symp. on Rock Joints*. Loen, Norway, Eds: N Barton and O Stephansson, Balkema, Rotterdam, 603 - 610.
- Barton N, Choubey V (1977). The shear strength of rock joints in theory and practice. *Rock Mech*, 10: 1-54.
- Baud P, Louis L, David C, Rawling GC, Wong T-f (2005). Effects of bedding and foliation on mechanical anisotropy, damage evolution and failure mode, *Geol. Soc. Lond. Special Publication*, 245: 223 - 249.
- Cai M, Kaiser PK, Tasaka Y, Minami M (2007). Peak and residual strengths of jointed rock masses and their determination for engineering design. *Proc of the 1st Canada-US Rock Mech. Symp.*, Vancouver, Canada, 1: 259 - 267.

Chong WL, Haque A, Ranjith PG, Shahinuzzaman A (2013). Modeling of intact and jointed mudstone samples under uniaxial and triaxial compression, *Arab J. Geosci.*, 6: 1639 – 1646.

Coulomb CA (1776). Essai sur une application des regles de maximis et minimis a quelques problemes de statique, relatifs al'architecture. *Memoires de Mathematique et de Physique*, presents a l'Academie, Royale des Sciences par divers Savans, 7: 343 - 382.

Dunn DE, Lafountain LJ, Jackson RE (1973). Porosity dependence and mechanism of brittle fracture in sandstone, *J. Geophys. Res.*, 78: 2403 - 2417.

Einstein HH, Veneziano D, Baecher GB, O'Reilly KJ (1983). The effect of discontinuity persistence on rock slope stability, *Int. J. Rock Mech. Min. Sci. Geomech. Abstr.*, 20: 227 - 236.

Grasselli G, Egger P (2003). Constitutive law for the shear strength of rock joints based on three-dimensional surface parameters, *Int. J. Rock Mech. Min. Sci.*, 40(1): 25 – 40

Haberfield CM, Johnston IW (1994). A mechanistically-based model for rough rock joints. *Int. J. Rock Mech. Min. Sci. Geomech. Abstr.*, 31(4): 279 - 292.

Halakatevakis N, Sofianos AI (2010). Strength of a blocky rock mass based on an extended plane of weakness theory, *Int. J. Rock Mech. Min. Sci.*, 47: 568 - 582.

Haque A, Kodikara J (2012). A simplified analytical model for predicting the shear behavior of regular triangular rock/concrete joints under constant normal stiffness, *Geotechnique*, 62(2): 171 - 176.

Hoek E, Carlos C, Brent C (2002). Hoek-Brown failure criterion-2002 Edition. *Proc of the NARMS-TAC Conference*. Toronto, 1: 267 - 273.

Hoek E, Kaiser PK, Bawden WF (1995). Support of underground excavations in Hard rock, A.A. Balkema, 215.

Homand F, Lefevre F, Belem T, Souley M (1999). Rock joints behavior under cyclic direct shear tests. In: *Rock Mechanics for Industry*, Eds: K Amadei, S Smealie, Balkema, Rotterdam, 399 – 406.

Jaeger JC (1959). The frictional properties of joints in rock. *Geofisica Pura e Applicata Maggio–Agosto*, 43(1): 148 - 158.

Jaeger JC (1971). Friction of rocks and the stability of rock slopes, Rankine Lecture. *Geotechnique*, 21: 97 - 134.

Jaeger JC, Cook NGW, Zimmerman RW (2007). *Fundamentals of Rock Mechanics*, 4th ed. Oxford: Blackwell.

- Kim BH, Cai M, Kaiser PK (2007b). Rock mass strength with non-persistent joints, Proc. of the 1st Canada-US Rock Mech. Symp., Vancouver, Canada, 1: 241 - 248.
- Kim BH, Kaiser PK, Grasselli G (2007a). Influence of persistence on behavior of fractured rock masses, Geol. Soc. Lond. Special Publications, 284: 161 - 173; Doi:10.1144/SP284.11.
- Kulathilake PHSW, Malama B, Wang J (2001). Strength predictions for jointed rocks in confined and unconfined states, Int. J. Rock Mech. Min. Sci., 38: 641 - 657.
- Kulathilake PHSW, Shou G, Huang TH, Morgan RM (1995). New peak shear strength criteria from anisotropic rock joints. Int. J. Rock Mech. Min. Sci. Geomech. Abstr., 32(7): 673 - 697.
- Kumar D, Das SK (2005). An experimental study of the parameters influencing ultimate bearing strength of weak floor strata using physical modeling, Geotech. Geol. Eng., 23: 1 - 15.
- Lee SW, Hong ES, Bae SI, Lee IM (2006). Modelling of rock joint shear strength using surface roughness parameter, Rs, Tunn. Undergr. Sp. Tech., 1: 21(3 - 4).
- Mohr O (1900). Welche Umstände bedingen die Elastizitätsgrenze und den Bruch eines Materials. Zeitschrift des Vereins Deutscher Ingenieure, 44: 1524 - 1530.
- Patton FD (1966). Multiple modes of shear failure in rock, Proc. of the 1st International Cong. on Rock Mech., Lisbon, 1: 509 - 515.
- Ramamurthy T, Arora VK (1994). Strength predictions for jointed rocks in confined and unconfined states, Int. J. Rock Mech. Min. Sci. Geomech. Abstr., 31: 9 - 22.
- Ranjith PG, Fourar M, Pong SF, Chian W, Haque A (2004). Characterization of fractured rocks under uniaxial loading states, Int. J. Rock Mech. Min. Sci., 41: 361 - 366.
- Saeb S (1990). A variance on Ladanyi and Archambault's shear strength criterion, Rock Joints, Ed: S. Barton, Balkema, Rotterdam, 701 - 705.
- Singh M, Rao KS, Ramamurthy T (2002). Strength and deformational behavior of a jointed rock mass, Rock Mech. Rock Eng., 35: 45 - 64.
- Tiwari RP, Rao KS (2004). Physical modeling of a rock mass under a true triaxial stress state, Int. J. Rock Mech. Min. Sci., 41(3): paper 2A 14.
- Wasantha PLP, Ranjith PG, Viete DR (2014). Effect of joint orientation on the hydro-mechanical behavior of singly jointed sandstone experiencing undrained loading, J. Geophys. Res.-Sol. Ea., 119(3): 1701 - 1717.
- Wasantha PLP, Ranjith PG, Haque A, Kodikara J, Bouazza A (2011). Implications of joint properties on the strength of a jointed rock mass, Advances in Unsaturated Soil, Geo-Hazard, and Geo-Environmental Engineering: pp. 258 - 266. doi: 10.1061/47628(407)33.

Xia CC, Tang ZC, Xiao WM, Song YL (2013). New peak shear strength criterion of rock joints based on quantified surface description. *Rock Mech. Rock Eng.*, DOI: 10.1007/s00603-013-0395-6.

Wasantha PLP, Ranjith PG, Viete DR (submitted). Hydro-mechanical behavior of sandstone with interconnected joints under undrained conditions. *Acta Geotech.*

Yang ZY, Chen JM, Huang TH (1998). Effect of joint sets on the strength and deformation of rock mass models, *Int. J. Rock Mech. Min. Sci.*, 35(1): 75 - 84.